2.2 Circuit Model Theory

This study uses a number of small compartment models such as the three-element windkessel model [34], and extensions of it [25], [31] to analyze blood pressure and blood flow velocity data during postural change from sitting to standing. Common for all these models is that they can be represented by electrical circuits with resistors, capacitors, and inductors. Model equations can be derived using theory from circuit analysis. In this analogy, voltage plays the role of blood pressure and current plays the role of flow.

Using such circuits, the pressure-flow behavior can be characterized by studying the system impedance, which is a frequency-domain relationship between the pressure and flow. Therefore, in order to adequately study and evaluate these models, it is useful to perform the analysis in the frequency domain. To enable the frequency-domain analysis of both the model and the measured data, steps are required that allow for the transformation from the time domain to the frequency domain. The method of Laplace transforms was selected to facilitate the analysis of the model. The Laplace transform provides a means for relating the time-domain behavior of a linear circuit to its frequency-domain behavior [16], [20], [23], [28]. Use of the Laplace transform and its properties allows us to transform the differential equation that results in our time-domain analysis of the circuit, to an algebraic equation in the frequency domain. The Laplace transform is defined by

$$F(s) = \mathcal{L}\{f(t)\} = \int_{0^-}^{\infty} f(t)e^{-st}dt.$$

This definition is called the *unilateral* or *one-sided* Laplace transform because the lower limit of the integral is 0. Values of $f(t)$ for $t < 0$ are ignored. Extending the lower limit of integration to $-\infty$ gives the *bilateral* or *two-sided* Laplace transform definition.

$$F(s) = \mathcal{L}\{f(t)\} = \int_{-\infty}^{\infty} f(t)e^{-st}dt. \tag{1.1}$$

In our case, the data is only defined for time $t \geq 0$, so if we extend the signal to $-\infty$ and let all values for $t < 0$ be equal to zero, the unilateral and bilateral Laplace transforms are the same. The Laplace transform variable s represents complex frequency and can be written as $s = \sigma + i\omega$, where σ denotes its real part and ω denotes its imaginary part. It can be shown that the Fourier transform is a special case of the bilateral Laplace transform when the real part of the complex frequency equals zero (i.e., $s = i\omega$). Fourier analysis is based on the decomposition of a signal into sine and cosine waves. The Fourier transform uses the sinusoidal waves of the decomposed signal to expose frequency-domain characteristics of the signal such as the harmonic content. By observing the frequency-domain dynamics (or frequency spectrum) of a periodic signal, the amplitude and phase of the harmonic terms can be identified. In keeping with the sinusoidal basis of Fourier analysis, the exponential term used in Fourier transformation must be in accordance with Euler's formula

$$e^{i\omega t} = \cos(\omega t) + i\sin(\omega t).$$

In the Laplace transform definition (equation (1.1)), an additional exponential term is present, since $e^{-st} = e^{-(\sigma+i\omega)t} = e^{-\sigma t}e^{-i\omega t}$. If we let $\sigma = 0$, then $s = i\omega$ and equation (1.1) becomes

$$F(s) = \int_{-\infty}^{\infty} f(t)e^{-i\omega t}dt, \tag{1.2}$$

which is written $F(\omega)$ since *s* is now a function of ω alone. Equation (1.2) corresponds to the Fourier transform of $f(t)$. Therefore, the Fourier transform is a special case of the bilateral Laplace transform.

Using the Laplace transform to analyze the circuit requires developing an *s*-domain equivalent circuit. This is done by transforming the individual circuit elements into

impedances. The *s*-domain impedance of a circuit element is written as $Z(s) = V(s)/I(s)$, where $V(s)$ is the *s*-domain value of the voltage across the circuit element and $I(s)$ is the *s*-domain value of the current through the element. To determine the impedances, we first write a time-domain equation relating the voltage and current of the element, and then we take the Laplace transform of the time-domain equation. Below are the steps for deriving the *s*-domain values of a resistor, inductor and capacitor. Before beginning, it should be noted that the Laplace transform of a voltage, *v(t)*, is written as *V(s)*, and that of a current, *i(t)*, is written as *I(s)*. Also, there are two properties of importance that we will be using in our derivations. Given the function $f(t)$ and its Laplace transform *F(s)*, the following are properties of the unilateral Laplace transform:

- Linearity: $\mathcal{L}\{Kf(t)\} = KF(s)$, for K constant.
- Differentiation: $\mathcal{L}\left\{\frac{df(t)}{dt}\right\} = sF(s) - f(0^-)$.

The Laplace transform and its properties are used to derive the impedances of the circuit elements below.

Resistor:

From Ohm's law we write the relationship $v(t) = Ri(t)$, where *R* (constant) is the resistance. Using the linearity property, the Laplace transform is easily obtained. We have $V(s) = RI(s)$ therefore the *s*-domain impedance of a resistor is given by $Z(s) = V(s)/I(s) = R$. Note that this is the same as the time-domain resistance. This will not be true for the other circuit elements.

Inductor:

The time-domain equation relating the voltage to the current of an inductor of L henrys carrying an initial current of I_0 amperes is $v(t) = Ldi(t)/dt$. Using the linearity and differentiation properties, the Laplace transform of the equation is found to be $V(s) = L\left[sI(s) - i(0^-)\right] = sL\left[I(s)\right] - LI_0$. Assuming an initial current of zero, we have $V(s) = sLI(s)$, and the impedance of the inductor is $Z(s) = V(s)/I(s) = sL$.

Capacitor:

The time-domain equation relating the voltage to the current of a capacitor of C farads with an initial voltage of V_0 volts is $i(t) = Cdv(t)/dt$. Using the properties listed above we find the Laplace transform of the equation to be $I(s) = C\left[sV(s) - v(0^-)\right] = sCV(s) - CV_0$. Assuming the capacitor is not initially charged, the equation becomes $I(s) = sCV(s)$, and the impedance of the capacitor is given by $Z(s) = V(s)/I(s) = 1/(sC)$.

A summary of the time-domain and *s*-domain values is shown in Table 1. Zero initial-condition values on the circuit elements are assumed. Also noted in the table are the *s*-domain values of the input voltage (in this case, the blood pressure, *p(t)*) and the current (the blood flow, *q(t)*).

Table 1: Model parameters and their *s*-domain equivalents.

Time Domain	*s*-Domain
R	R
C	$\frac{1}{sC}$
L	sL
$p(t)$	$P(s)$
$q(t)$	$Q(s)$

Once all the circuit elements have been transformed to their *s*-domain equivalents, we can reduce the impedances to a single equivalent impedance for the model. The purpose for doing this is to establish a relationship that can be used to evaluate the model based on the measured data. In our models, flow *Q(s)* plays the role of current, pressure *P(s)* plays the role of voltage, consequently, impedance can be defined by

$$Z(\omega) = \frac{P(\omega)}{Q(\omega)}. \tag{1.3}$$

For each circuit, the impedance will be determined by combining the individual circuit element impedances in series or in parallel. Impedances are combined the same way resistors are combined. For two impedances, Z_1 and Z_2, in series, the combined impedance is $Z_1 + Z_2$. Impedances in parallel can be combined as $\frac{1}{Z_1} + \frac{1}{Z_2}$ or as $\frac{Z_1 Z_2}{Z_1 + Z_2}$.

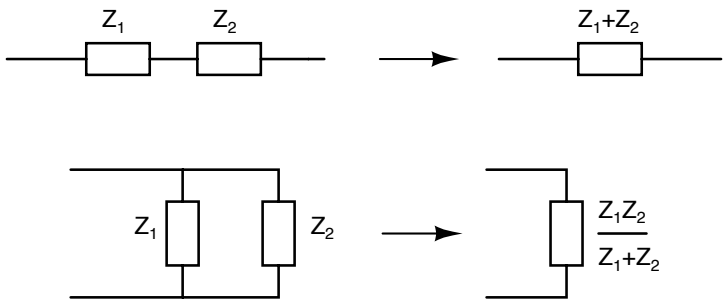

Figure 2: Combined impedances in series (top) and in parallel (bottom).

Using this theory, we can derive an equation for the impedance of the model. This impedance is dependant on the values of the circuit elements (resistors, capacitors, inductors). Therefore, those parameter values must be determined.

2.3 The Discrete Fourier Transform

The impedance of the measured data can be computed by calculating the Fourier Transform of the measured blood pressure $p_F(t)$ and flow $q_{MCA}(t)$ to create their respective frequency-domain equivalents, $P_F(\omega)$ and $Q_{MCA}(\omega)$. The ratio of these two gives the impedance of the data, as is indicated in equation (1.3). The measured impedance is denoted $Z_M(\omega)$. The pressure and flow measurements are periodic sequences of values obtained by sampling a continuous-time signal. To perform computational frequency-domain analysis involving sampled signals, the discrete Fourier transform (DFT) is used. The DFT is a Fourier transform that can be calculated from a finite set of discrete-time samples of an analog signal and which produces a finite set of discrete-frequency spectrum values [20], [23], [28]. The DFT, and more specifically the Fast Fourier Transform (FFT) algorithm that implements the DFT, is useful because it is well suited for computer calculation. As the definition below shows, the DFT relates the discrete-time sequence $x[n]$, $n=0,\ldots,N-1$ to the discrete-frequency sequence $X[k]$, $k=0,\ldots,N-1$.

$$X[k] = \sum_{n=0}^{N-1} x[n] e^{-i 2\pi k n / N}$$

To convert the signal from the frequency domain back to the time domain, the inverse DFT is used. It is defined as

$$x[n] = \frac{1}{N} \sum_{k=0}^{N-1} X[k] e^{i 2\pi k n / N} .$$

For our purposes, the fft and ifft functions in MATLAB are used to perform the computations to and from the frequency domain. The algorithms used for both commands are similar, employing the Cooley-Tukey algorithm to recursively decompose the DFT into smaller DFTs [14].

Of particular importance in DFT analysis is the number of samples *N* in the data segment that is being transformed. The resolution of the frequency spectrum, or the frequency interval between data points, is determined by *N*. The frequency resolution is calculated as f_s/N, where f_s is the sampling frequency that was used to create the sampled signal. The closer the data points are together, the denser the resolution, therefore it can be advantageous to decrease f_s/N by increasing *N* [20], [23], [28]. Analysis of a signal can be done by splitting it up into shorter segments, and then taking the DFT of each segment. An additional step, which can have the affect of smoothing or otherwise shaping the resulting spectrum, is the application of a window function, *w(t)*, prior to taking the DFT. The window is a function of time that is multiplied by the data segment, and the resulting product is then transformed. A rectangular or box window is, in essence, the function *w(t)*=1 over the interval of the data segment. The abrupt cutoff at the edges of the rectangular window can have undesirable effects such as the generation of side lobes in the frequency spectrum; therefore several functions have been developed that produce a modified window shape in order to provide smoother results. Some examples are the 10% cosine taper function, the Hamming function, and the Hanning function, which all produce windows based on the shape of the cosine waveform. The Hanning window is commonly used in analysis of hemodynamics [4], [13].

When studying blood pressure and flow data, one method of analysis is to use the FFT to perform calculations on a beat-to-beat basis, meaning the segment sizes will be related to the cardiac cycle as it is observed in the data. We will refer to a cardiac cycle as one period. Since cardiac cycles do not have a uniform time length, *N* will vary throughout the DFT calculations of the data. Since *N* varies by period, each period will have a different

frequency resolution. The data segment can be increased to include multiple cardiac cycles (i.e. multiple periods). When this is done, it is useful to perform calculations using overlapping segments.

Another DFT method that has been used in previous studies is the windowed Fourier transform (WFT) [19]. Also called the short-time Fourier transform (STFT), it differs from the FFT in that a single window size is used for all frequencies, meaning each segment will have the same number of samples. As such, the resolution of the analysis is the same at all locations in the time-frequency domain. In effect, the window function, $w(t)$ slides along the input signal $x(t)$, and the product of the two is transformed. For each shift $w(t-s)$, the Fourier transform of $x(t)w(t-s)$ is computed. Any of the window functions mentioned above can be applied to this method [20], [23], [28].

2.4 The Three-Element Windkessel Model

The initial method used to analyze the measured data for blood pressure and blood flow velocity is the classical three-element windkessel model which is frequently used in cardiovascular studies [4], [11], [19], [30], [33]. This model, conceived by Westerhof, et al. [34], is an extension of the two-element windkessel model introduced by Otto Frank in 1899 [7]. Frank's model was based on the comparison of the heart pumping blood into the arterial tree with the hand-pumped fire engine, where water is pumped by periodic injections into a high-pressure air-chamber ("windkessel" in German) to provide continuous outflow from the water hose. The whole arterial tree is modeled as an elastic chamber with a constant compliance and a resistance representing the total resistance of the arterial tree. The electrical equivalence is a parallel connection of a capacitor and a resistor. The three-

element model comprises an additional resistor in series with the two-element model. This component represents characteristic impedance, and it is based on wave-transmission theory. This term allows for better interpretation of the transformation of the pressure and flow pulses as they travel to the periphery. Whereas the two-element windkessel is limited in its utility to very low frequencies, the three-element model has the capacity to provide better results at higher frequencies [31]. In our study, we assume that the resistor R_1 [mmHg·s/cm^3] and the capacitor C [cm^3/mmHg] represent the systemic resistance and compliance of the arteries leading to and including the middle cerebral artery (MCA). The other resistor, R_2 [mmHg·s/cm^3], represents the resistance associated with the peripheral cerebrovascular bed. We use blood pressure as an input to the model to predict blood flow. However, since pressure in the brain cannot be measured non-invasively, we use the Finapres measurements of arterial pressure in the finger (p_F [mmHg]) as the input to the model. The fast propagation of the pressure wave and the relatively small dispersion allows us to use arterial blood pressure measurements in our analysis. The use of finger pressure is what makes the lumped model in some way represent the entire systemic response. The output from the model is the volumetric flow rate (q_{MCA} [cm^3/s]) in the MCA. It should be noted that the measurements provide data for velocity in the MCA, not blood flow (volumetric flow rate), which the windkessel model provides. Blood flow is obtained assuming a constant radius of $r = 0.2$ cm. The radius of the MCA varies among the different subjects, but we assume it to be constant because direct measurements of the radius are not available. Using this radius, we let the blood flow be $q = \pi r^2 v$ [cm^3/s] where v [cm/s] is the blood flow velocity. All data shown in the results sections are based on blood flow rather than blood flow velocity.

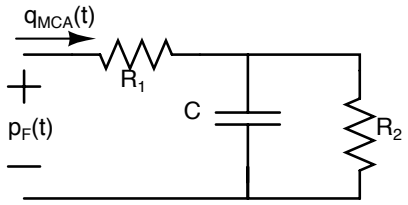

Figure 3: The three-element windkessel model with two resistors R_1 and R_2 and a capacitor marked by C. The finger blood pressure $p_F(t)$ is represented as voltage, and the blood flow in the MCA $q_{MCA}(t)$ is current.

Using equation (1.3) the impedance of the model is given by $Z_M(\omega) = P_F(\omega)/Q_{MCA}(\omega)$, where $P_F(\omega)$ and $Q_{MCA}(\omega)$ are the transforms of the pressure and flow data. The efficacy of the model will be evaluated in two ways: by comparing the predicted flow of the model $q(t)$ with the measured flow data $q_{MCA}(t)$; and by comparing the impedance magnitude of the model $Z_W(\omega)$ with the measured impedance $Z_M(\omega)$.

To derive the equation for the model impedance we must analyze our circuit model (Figure 3) in the frequency domain. The circuit elements are transformed using Table 1. The impedances of the resistors are just R_1 and R_2, and the impedance of the capacitor is $1/(sC)$. Now we use the circuit analysis technique of combining impedances in parallel to reduce the circuit as shown in Figure 4. We obtain an equivalent impedance for $R_2 \,\|\, 1/(sC)$.

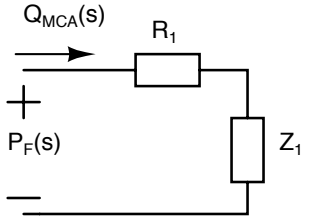

Figure 4: The reduced circuit model shown in the frequency domain. R_2 and $1/(sC)$ have been combined in parallel to give the equivalent impedance, Z_1.

Hence, the impedance Z_1 is given by

$$Z_1 = R_2 \,||\, \frac{1}{sC} = \frac{R_2 \dfrac{1}{sC}}{R_2 + \dfrac{1}{sC}} = \frac{R_2}{sR_2C + 1}.$$

Finally, the overall circuit impedance is determined by combing the remaining impedances in series.

$$Z_W(s) = R_1 + Z_1 = R_1 + \frac{R_2}{1 + sCR_2} = \frac{R_1 + R_2 + sCR_1R_2}{1 + sCR_2} \quad \Leftrightarrow$$

$$Z_W(\omega) = \frac{R_1 + R_2 + i\omega CR_1R_2}{1 + i\omega CR_2}, \qquad s = i\omega. \tag{1.4}$$

As mentioned earlier, the Fourier transform is a special case of the bilateral Laplace transform when $s = i\omega$. Therefore, by setting $s = i\omega$ we have essentially determined the equation of the Fourier transform of the impedance of our model. This equation, when set equal to equation (1.3), gives us the relationship between blood pressure, flow, and impedance.

The impedance of the data is obtained using FFT to determine the Fourier transform of the pressure data and the flow data, and then taking the ratio of the two. The maximum frequency of the impedance spectrum that can be calculated is determined by the sampling rate. The sampling theorem states that the maximum frequency must be no greater than one half the sampling frequency. Our data was sampled at a rate of 50 Hz, therefore the impedance spectrum can be calculated up to 25 Hz. We have chosen to plot the impedance up to 10 Hz, which provides us with the useful information we need and also reduces aliasing [4] (see Figure 5). The beat-to-beat method of analysis is conducted in this study. Therefore the segment sizes are based on the cardiac cycle, where each cycle represents one period. In

order to determine the best estimation of the model, we perform the FFT calculations using segment sizes of 1, 2, 4, and 8 periods. Since our method uses the cardiac cycle as a reference for the periods, it is necessary to separate the time series at the beginning of each cardiac cycle. A matrix is created that has in its rows that pressure data for each one of the periods. A similar matrix is created for the flow data. We also create a matrix containing the corresponding time values for each of the measured data points. With the data formatted in this way, the FFT computations are easily conducted. A rectangular window is used in this analysis. We obtain results from analyzing one period of data at the time, as well as results from analyzing overlapping segments of 2, 4, and 8 periods. What this means is that two/four/eight periods are modeled at a time, then there is a shift of one period, and the next two/four/eight periods are modeled. For example, for two period segments, the model is computed for periods {1,2}, then {2,3}, then {3,4}, etc. Likewise, for four periods, the model is computed for periods {1,2,3,4}, then {2,3,4,5}, then {3,4,5,6}, etc. The process is the same for eight period segments. In this way we are able to compile results and monitor how they change throughout the entire duration of the postural change of the subject. The reason the calculations were done over multiple segment sizes is that it can provide different views of the frequency spectrum based on different frequency resolutions. For larger segment sizes, the value of N is larger and a higher frequency resolution is obtained. For example, consider a data segment consisting of four cardiac cycles, where the consecutive cycle lengths are 1.1 sec, 0.9 sec, 1.0 sec, and 1.2 sec. The measured data were sampled at 50 Hz, so for the first period there are $1.1 \text{ sec} \times 50 \text{ Hz} = 55$ data points. The number of samples in the remaining three periods are, respectively, 45, 50, and 60. If we use a segment size of one period to calculate the FFT, we have $N = 55$, which corresponds to a frequency

resolution of $50\ \text{Hz}/55 = 0.91\ \text{Hz}$. Extending the segment size to two periods, there are 55+45=100 data points, so the frequency resolution is $50\ \text{Hz}/100 = 0.5\ \text{Hz}$. Further extending the segment to include all four periods increases N to 210 and results in a frequency resolution of 0.24 Hz. An example of the different results that are obtained when the FFT is computed for the various segment sizes is shown in Figure 5. An 8-period portion of the flow data *q(t)* is presented, and the magnitudes of the resulting Fourier transforms $|Q(\omega)|$ are shown. The four curves in the frequency spectrum correspond to the FFT being computed over 4 different segments: the first period on the graph; the first two periods; the first four periods; and all 8 periods.

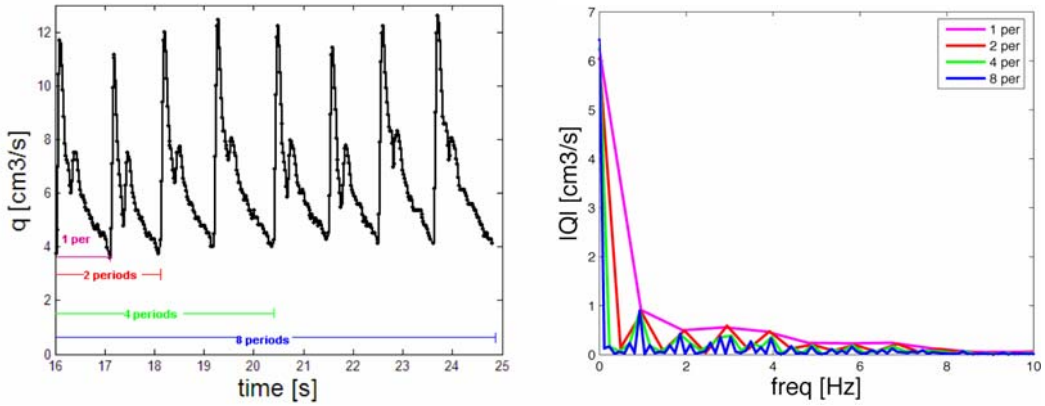

Figure 5: Measured flow plotted in the time domain and in the frequency domain over 8 periods. The left panel shows an 8 period window of the measured flow data and the right panel shows the corresponding frequency spectrum obtained using the FFT.

Once the Fourier transforms of the pressure and flow data have been computed, the measured impedance is calculated. Figure 6 shows examples of typical impedance magnitude plots for each of the three subject types using a single period during sitting.

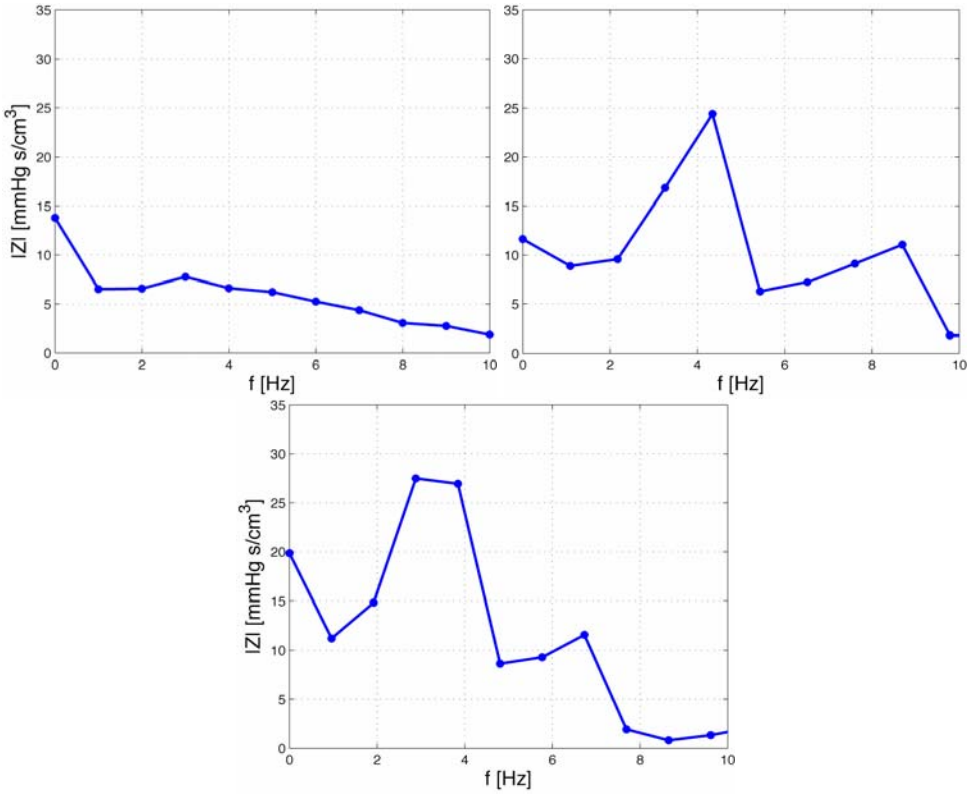

Figure 6: Measured impedance plots for healthy young (top left), healthy elderly (top right), and hypertensive elderly (bottom) subjects during sitting. A single period was used.

As a means of evaluating the model, we will compare the measured impedance and the model impedance and attempt to minimize the error between the two. In order to achieve this, we must identify the three model parameters, R_1, R_2, and C.

Methods of parameter estimation have been explored in many studies [12], [19], [24], [26], [30]. The accuracy of the estimates has also been examined [6], [24]. It has been found that the three-element windkessel model tends, in general, to overestimate the value of C and underestimate the value of R_1. However, it has also been found that when the model is used to fit experimental pressure and/or flow data, it can produce realistic results but the estimated parameter values deviate significantly from the actual values [6], [25]. When the objective is to estimate the parameter values as accurately as possible, the model no longer produces the

realistic pressure and flow wave shapes. This discrepancy is related to the fact that the characteristic impedance, represented by the resistance R_1, in series with the parallel combination of C and R_2, does not directly correlate to physical properties, particularly at low frequencies. This issue was addressed in the development of new models by adding an inertance element to counteract the effect of the resistance at low frequencies [25], [33]. In our case, the objective is to evaluate the performance of the model in terms of how the impedance and flow compare to actual data, therefore we focus on obtaining the best results from the model rather than trying to optimize parameter value accuracy. Our parameter-estimation methods are based on fitting the magnitude of the impedance for the model to the magnitude of the impedance of the measured data.

For the three-element windkessel model, we implemented two different methods for determining the value of C, while using the same values of R_1 and R_2 , which are readily obtained from the measured impedance as is described below. For both methods of estimating C, we evaluate the model and determine how the methods differ. All parameters were determined as a function of time so that we have a representation of the dynamic changes of the parameters during postural change.

The values of R_1 and R_2 were obtained by observing the zero- and high-frequency limits of the model impedance. For the three-element windkessel model, both of these limits result in impedances dependant only on the resistances.

$$\lim_{\omega \to 0} Z_W(\omega) = R_1 + R_2$$

$$\lim_{\omega \to \infty} Z_W(\omega) = R_1.$$

These equations are easily verified by observing the circuit model. At low frequencies the capacitor acts as an open circuit, and the model becomes a two-element circuit of R_1 and R_2

in series. At high frequencies the capacitor acts as a short circuit, eliminating the affect of R_2. The relationship produced by the zero-frequency limit indicates that the value $R_1 + R_2$ corresponds to the direct current (DC) value of the impedance. By fitting the model to the measured impedance we get $Z_M(0) = R_1 + R_2$, therefore $R_1 + R_2$ is obtained directly by picking out the DC value of Z_M. The high-frequency limit corresponds to the value of the measured impedance at the highest meaningful frequency. Due to the significant noise content in the data, it works better to approximate the high-frequency limit by taking the mean value of the measured impedance over a number of high frequencies. It was determined through investigation that the value of R_1 is best chosen as the mean of Z_M over frequencies from 3- 8 Hz [19].

The first estimation of C uses the low-frequency impedance method which was proposed by Laskey et al [12], and is used in [19], [26]. The magnitude of the impedance $|Z|$ is analyzed as a function of frequency. The point at which the two impedance curves (impedance of the data and impedance of the model) first cross each other is estimated to be between the 2nd and 3rd data points of the measured impedance. The magnitude of the measured impedance at this point is denoted $\left|Z_M(\omega_{2,3})\right|$ and can be written in terms of the 2nd and 3rd data points

$$\left|Z_M(\omega_{2,3})\right| = \frac{\left|Z_M(\omega_2)\right|}{2} + \frac{\left|Z_M(\omega_3)\right|}{2}.$$

Likewise, the frequency $\omega_{2,3}$ can be written in terms of the frequency at the 2nd and 3rd data points

$$\omega_{2,3} = \frac{\omega_2}{2} + \frac{\omega_3}{2}.$$

Now we use equation (1.4) to develop an equation for the magnitude of the impedance of the model

$$|Z_W|^2 = \frac{(R_1 + R_2)^2 + (\omega R_1 R_2 C)^2}{1 + (\omega R_2 C)^2}.$$

By inserting the values for $\omega_{2,3}$ and $|Z_M(\omega_{2,3})|$ we obtain an equation that yields a value for C based on the values of R_1 and R_2

$$C = \frac{1}{\omega_{2,3} R_2} \sqrt{\frac{(R_1 + R_2)^2 - |Z_M(\omega_{2,3})|^2}{|Z_M(\omega_{2,3})|^2 - R_1^2}}.$$

As seen in this equation, if $|Z_M(\omega_{2,3})|$ is less than R_1, a value of C does not exist. This is a major limitation of this method of parameter estimation. It is of particular concern for us when we use segments of more than one period to conduct our analysis because in those cases the effects of noise and harmonics on the impedance spectrum are significantly more pronounced than they are in the impedance spectrum resulting from 1-period analysis (which is shown in Figure 6). The measured impedance curves from multiple-period analysis contain spikes throughout the entire frequency range, which affect the calculations of both R_1 and $|Z_M(\omega_{2,3})|$, making it difficult to get accurate results for C.

The second method for determining C uses the MATLAB function fminsearch to find the optimum value. Fminsearch is a Nelder-Mead simplex algorithm that performs unconstrained nonlinear optimization, finding the minimum of a scalar, multivariate function. It minimizes the objective function by iteratively calling the function until the optimum values of the variables are reached within a specified tolerance. The algorithm uses the concept of a simplex, which is a polytope of $n+1$ vertices where n is the number of

parameters. At each step of the search a new point is generated in or near the current simplex. The function is evaluated at each of the $n+1$ vertices, and the point that gives the worst result is then replaced by a new point. This is repeated until the specified tolerance is reached. For our purposes, the function to be minimized is a cost function that calculates the sum of square differences between the measured impedance and model impedance over all frequency points in the current segment. Since we have already determined R_1 and R_2 , the cost function only has one parameter, C, to optimize. The initial value of C comes from the typical values mentioned in Toy et al [31].

Having determined the parameters in the windkessel model, we use equation (1.4) to compute the impedance of the model, Z_W. Furthermore, we can use this impedance to calculate the flow so that the results of the model may be validated. The flow is calculated by manipulating equation (1.3) to get $Q_{MCA}(\omega) = P_F(\omega) / Z_W(\omega)$, and then implementing the inverse FFT. This produces a time-domain function, which is compared to the measured flow data for validation.

These techniques were used to analyze the measured data from three different subject groups: healthy young subjects, healthy elderly subjects, and hypertensive subjects. Results were collected for all three groups.

2.5 Higher-Order Models

Four additional models were analyzed using the same methods as discussed above. The development of extensions to the classical three-element windkessel model is fueled, in part, by the desire for the model impedance to better resemble the actual system impedance [31]. Another driving force is the need for more accurate parameter estimation [25], [33]. It

has been noted that one of the shortcomings of the original three-element model is its inability to reproduce some of the principal features that occur in measured impedance [2], [31]. The fluctuations, or "bumps" that occur in the low to medium frequencies of the magnitude of the measured impedance (seen for all three subject types in Figure 6), cannot be described with a first-order model such as the classical three-element model. In order to replicate these relative maxima and minima, modifications to the model have been studied. All of the models that are analyzed here are based on the design of the original three-element model. They differ in that the configuration and/or number of parameters have been adjusted. We still work under the assumption of model linearity, and are able to enforce the same circuit analysis and frequency domain analysis techniques. The models have been selected from studies of windkessel model extensions [25], [31], [33]. These models were originally developed to study the arterial system, where aortic pressure and flow were the signals being analyzed. The circuit diagrams of the models are shown in Figures 7-10, and the corresponding impedances of the models, as well as the zero- and high-frequency limits are shown in Table 2.

The 3-element model #2 (Figure 7) was proposed by Toy et al [31], and differs from the original model that was discussed in that the circuit elements are configured differently. The four-element model, shown in Figure 8, was first proposed by Burattini and Gnudi [3] and is studied in [24], [25]. This model was developed to address the concept of system inertia, which is missing in the original three-element model. By placing an inductor in parallel with the impedance Z_0, the inertia of the system is accounted for. With this parallel arrangement, the inertia comes into play at low frequencies (in circuit analysis the inductor shorts out Z_0), and at high frequencies Z_0 dominates the impedance of the system (because

the inductor acts as an open circuit). This produces a model that more accurately replicates physical properties. As such, parameter estimation is more accurate with the 4-element model [25]. Although the four-element model achieves improvement over the three-element model in the accuracy of parameter estimation, it does not offer a much better fit of the system impedance [31]. The five-element models #1 and #2, shown in Figures 9-10, specifically address the objective of producing a model impedance that best represents the impedance of the measured data. In both models, the lumped compliance of the entire system is split up into two capacitors. The capacitors are separated by an inertance element. The difference between these two models is the placement of Z_0. The complexity of the impedance equations for these models provides the capability of describing the features of the impedance in more detail.

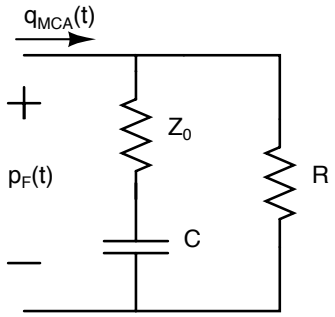

Figure 7: The three-element model #2. This model contains two resistors, R and Z_0 and a capacitor, C. It has the same components as the original three-element model, but in a different configuration. In this model and the models in Figures 8-10, the finger blood pressure $p_F(t)$ is represented as voltage, and the blood flow in the MCA $q_{MCA}(t)$ is current.

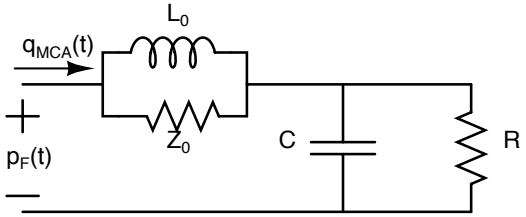

Figure 8: The four-element model. This model contains two resistors, R and Z_0, a capacitor, C, and an inductor, L_0.

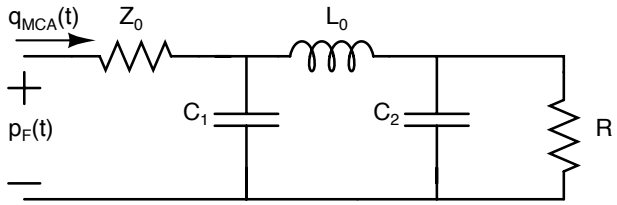

Figure 9: The five-element model #1. This model contains two resistors, R and Z_0, two capacitors, C_1 and C_2, and an inductor, L_0.

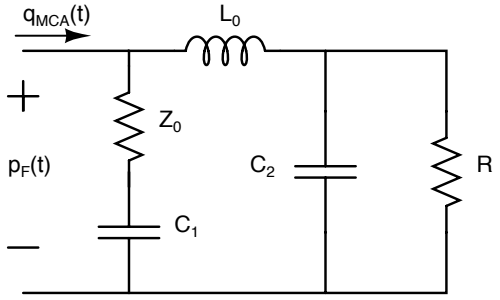

Figure 10: The five-element model #2. This model contains two resistors R and Z_0, two capacitors, C_1 and C_2, and an inductor, L_0. It has the same components as the five-element model #1, but in a different configuration.

Table 2: Impedance and limit equations for the 3, 4, and 5 element models.

Model	**Impedance of the model (Z_W)**	**Limit equations**
3-elmt#2 (Fig. 7)	$Z_W(\omega) = \dfrac{R + i\omega R Z_0 C}{1 + i\omega C(R + Z_0)}$	$\lim_{\omega\to 0} Z_W(\omega) = R$ $\lim_{\omega\to\infty} Z_W(\omega) = \dfrac{RZ_0}{R + Z_0}$
4-elmt (Fig. 8)	$Z_W(\omega) = \dfrac{RZ_0 - \omega^2 RZ_0 L_0 C + i\omega L_0(R + Z_0)}{Z_0 - \omega^2 RL_0 C + i\omega(RZ_0 C + L_0)}$	$\lim_{\omega\to 0} Z_W(\omega) = R$ $\lim_{\omega\to\infty} Z_W(\omega) = Z_0$
5-elmt#1 (Fig. 9)	$Z_W(\omega) = \dfrac{Z_0 + R - \omega^2 Z_0 L_0 C_1 - \omega^2 RL_0 C_2 + i\omega(L_0 + RZ_0 C_1 + RZ_0 C_2 - \omega^2 RZ_0 L_0 C_1 C_2)}{1 - \omega^2 L_0 C_1 + i\omega(RC_2 + RC_1 - \omega^2 RL_0 C_1 C_2)}$	$\lim_{\omega\to 0} Z_W(\omega) = Z_0 + R$ $\lim_{\omega\to\infty} Z_W(\omega) = Z_0$
5-elmt#2 (Fig. 10)	$Z_W(\omega) = \dfrac{R - \omega^2 L_0[RC_2 + Z_0 C_1] + i\omega[L_0 + RZ_0 C_1 - \omega^2 RZ_0 L_0 C_1 C_2]}{1 - \omega^2 C_1[RZ_0 C_2 + L_0] + i\omega[RC_1 + Z_0 C_1 + RC_2 - \omega^2 RL_0 C_1 C_2]}$	$\lim_{\omega\to 0} Z_W(\omega) = R$ $\lim_{\omega\to\infty} Z_W(\omega) = Z_0$

As shown in the Table 2, the low- and high-frequency impedance limits are all dependant only on resistances. Once again, this can be verified by observing the circuit

models and recalling the behavior of capacitors and inductors based on frequency. At zero frequency an inductor acts as a short circuit and a capacitor becomes an open circuit. The reverse is true at high frequencies: inductors behave like open circuits and capacitors are short circuits. The results of the zero-frequency equations are set equal to the DC value of the measured impedance. The high-frequency limit, like R_1 in the original three-element model, is obtained by taking the mean of Z_M over frequencies from 3-8 Hz. For the models shown in Table 2, we used the fminsearch function to come up with estimations of all parameters that are not determined from the limit equations. Depending on the model, if a parameter could be written as a function of another parameter, this was done so as to reduce the number of parameters to be optimized. The initial parameter values that were used as starting points for the algorithm were obtained either from the zero- and high-frequency limit equations or from the typical values mentioned in Toy et al [31]. In general, the initial resistance values in each of the models came from the limit equations, while the capacitance and inductance initial values were taken from [31]. The parameters were estimated on a beat-to-beat basis. The impedance of the model, based on the estimated parameters, was compared to the measured impedance. Flow was calculated for each model by taking the ratio of the impedance of the model and the Fourier transform of the measured pressure, which yields the frequency-domain flow value. This was then transformed to a time-domain result by taking the inverse Fourier transform, and it was compared with the measured flow data.